Polarization-resolved simulations of multiple-order rainbows using realistic raindrop shapes

Mathematical supplement

Alexander Haußmann - updated Oct 20th, 2020

Part I: GO model workflow

The following documentation presents the main calculation steps involved in the GO model for 2HS drop shapes, in order to provide a deeper insight in the polarization coordinate system definitions and the tracing of the Stokes vectors. It is not intended to be exhaustive; readers who are interested in the details should consult the Matlab source code instead, which will be provided by the author on request.

1. Drop shape

The 2HS drop surface is defined by two spheroid equations:

$$\frac{x^2+y^2}{a^2}+\frac{z^2}{b_1^2}=1 \qquad 0 \le z \le b_1$$

$$\frac{x^2+y^2}{a^2}+\frac{z^2}{b_2^2}=1 \qquad -b_2 \le z \le 0$$

with z being the direction of the semi-minor axes (Fig. 1), as long as $a > b_1 > b_2$. This is always the case for the equilibrium shape of water drops. This inequality might however be violated for transient stages of drop oscillations in the (2,0) mode [37]. Other modes of oscillations cannot be described with the 2HS model at all.

2. Incident sunlight

The direction of the incident sunlight from the center of the sun's disk at elevation h_S from the horizon (x, y-plane) is described by the unit vector $\vec{e}_{00}$:

$$\vec{e}_{00} = \begin{pmatrix} \cos h_S \\ 0 \\ -\sin h_S \end{pmatrix}$$

To account for the finite angular radius r_S of the sun, random points (indexed "SP") are chosen on the sun's disk by generating:

$\alpha'_{SP} = 2\pi \cdot \rho_1$ (sun disk centered azimuth)

$\zeta'_{SP} = (1 - \cos r_S) \cdot \rho_2 + \cos r_S$ (cosine of sun disk centered polar distance angle)

ρ_1 and ρ_2 are random numbers uniformly distributed between 0 and 1. These sun-disk-centered angular coordinates are transformed into angular coordinates in the *x, y, z* -system:

$$h'_{SP} = \arcsin \zeta'_{SP}$$

$$h_{SP} = \arcsin\left(\sin h'_{SP} \cdot \sin h_S - \cos h'_{SP} \cdot \cos h_S \cdot \cos \alpha'_{SP}\right)$$

$$\sin \alpha_{SP} = -\sin \alpha'_{SP} \cdot \frac{\cos h'_{SP}}{\cos h_{SP}}$$

$$\cos \alpha_{SP} = -\frac{\sin h'_{SP} - \sin h_{SP} \cdot \sin h_S}{\cos h_{SP} \cdot \cos h_S}$$

The unit vector for the incident light stemming from the point on the sun's disk selected by ρ_1 and ρ_2 is then given by:

$$\vec{e}_0 = \begin{pmatrix} -\cos h_{SP} \cdot \cos \alpha_{SP} \\ -\cos h_{SP} \cdot \sin \alpha_{SP} \\ -\sin h_{SP} \end{pmatrix}$$

This procedure models a disk with uniform emission power per solid angle element on this disk, from the center to the edge. Due to the small angular radius of the sun ($r_S \approx 0.27°$), the direction $\vec{e}_0$ differs only slightly from $\vec{e}_{00}$.

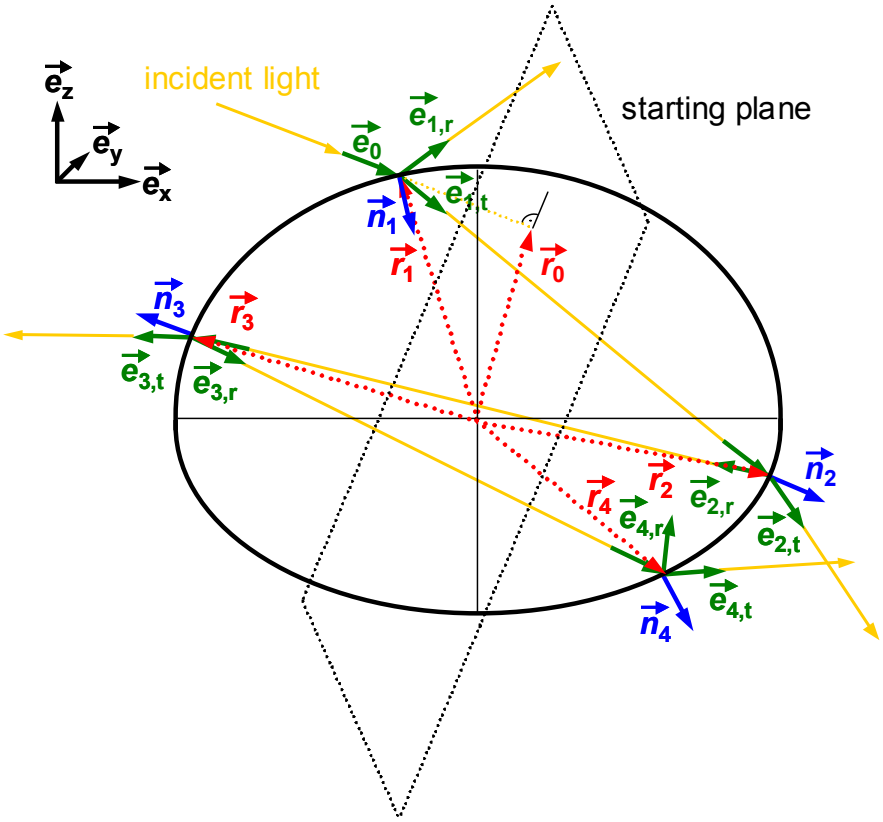

Fig. S1: Ray tracing through a 2HS shaped water drop. $\vec{r}_0$ *is chosen randomly on the starting plane perpendicular to* $\vec{e}_0$*. From this, the piercing points* $\vec{r}_1 \ldots \vec{r}_7$ *are calculated (only the first four are shown here). This is accomplished by calculating the respective propagation direction* $\vec{e}_{1,t}$, $\vec{e}_{2,r}$,... *of the ray through the drop from the laws of refraction and reflection in vectorial form, using the respective surface normal directions* $\vec{n}_1$, $\vec{n}_2$,... *At each interaction point, the intensity and polarization of the exiting rays* $\vec{e}_{1,r}$, $\vec{e}_{2,t}$,... *are evaluated.*

3. Starting point

The starting point $\vec{r}_0$ is chosen randomly on a plane perpendicular to $\vec{e}_0$ through the origin (see Fig. S1):

$$\vec{r}_0 = \max(a, b_1, b_2) \cdot \begin{pmatrix} \rho_4 \cdot \sin h_S \\ \rho_3 \\ \rho_4 \cdot \cos h_S \end{pmatrix}$$

ρ_3 and ρ_4 are random numbers uniformly distributed between –1 and +1. Under normal circumstances (no prolate drops), the prefactor will be equal to a. By this, it is guaranteed

that each element of the projected cross section area will be hit by the same amount of rays, i.e. that the effective ray density remains constant. Inevitably, some of these starting points will not lie within the drop's cross section (approximately 21.5% for a spherical drop), these are identified and sorted out during the next step. Of course, when multiple drop sizes are considered, the number of rays per drop size category has to be adjusted properly ($\propto a^2$) in order to keep the ray density per absolute area constant.

4. First piercing point and direction of the surface normal

Backtracking from $\vec{r}_0$ against the $\vec{e}_0$ direction yields the first piercing point $\vec{r}_1$, i.e. the physical incidence point of the ray on the sunward side of the drop, if the starting point was located inside the effective cross section. This can be determined from the set of solutions of the vectorial equation system comprising the straight line from $\vec{r}_0$ and the 2HS surface.

A critical issue of these calculations is the case discrimination between the upper and lower part of the 2HS drop, which is accomplished as follows: Assuming $b_1 > b_2$ (as usually fulfilled), the calculation is at first performed for a full spheroid with semi axes a and b_1. If the *z*-component of $\vec{r}_1$ turns out negative, it is clear that $\vec{r}_1$ must either lie on the lower part, or no such point exists (as the lower part is smaller, and can thus easier been missed). The calculation is in this case repeated for a full spheroid with semi axes a and b_2. The same method is applied for the determination of all subsequent piercing points.

The direction of the surface normal oriented towards the transmitted ray, i.e. into the drop, is then given by:

$$\vec{N}_1 = \begin{pmatrix} x_1 \\ y_1 \\ \left(a/b_{1,2}\right)^2 \cdot z_1 \end{pmatrix} \qquad \vec{n}_1 = -\frac{\vec{N}_1}{\left|\vec{N}_1\right|}$$

"$b_{1,2}$" means that the proper semi axis value has to be chosen depending on whether $\vec{r}_1$ is situated on the upper or lower part of the drop.

5. Initial Stokes vector

When a linear polarizer is rotated in 45° steps around the propagation direction of a light ray, the intensities $I_{-45°}$, $I_{0°}$, $I_{45°}$ and $I_{90°}$ can be measured successively. Moreover, the right- and left-handed circular intensities I_{RC} and I_{LC} can be measured as well through suitable filters. These data can be combined into the Stokes vector, which contains all information about the intensity and polarization state:

$$\vec{S} = \begin{pmatrix} S_0 \\ S_1 \\ S_2 \\ S_3 \end{pmatrix} = \begin{pmatrix} I_{0°} + I_{90°} \\ I_{0°} - I_{90°} \\ I_{45°} - I_{-45°} \\ I_{RC} - I_{LC} \end{pmatrix}$$

Of course, the different angular directions need a proper definition to make the Stokes vector concept applicable to the rainbow simulations. For the incident light, it is useful to construct the polarization coordinate system or "reference frame" in terms of unit vectors from the propagation direction $\vec{e}_0$ and the vertical direction $\vec{e}_z$, as long as $h_{SP} \neq \pm 90°$ (see Fig. S2):

$$\vec{e}_{0,0°} = \frac{\vec{e}_z \times \vec{e}_0}{\left|\vec{e}_z \times \vec{e}_0\right|}$$

$$\vec{e}_{0,90°} = \vec{e}_0 \times \vec{e}_{0,0°}$$

For the central point of the sun's disk ($\vec{e}_0 = \vec{e}_{00}$), the results are (Fig. S3):

$$\vec{e}_{0,0°} = \vec{e}_y = \begin{pmatrix} 0 \\ 1 \\ 0 \end{pmatrix} \qquad \text{and} \qquad \vec{e}_{0,90°} = \begin{pmatrix} \sin h_S \\ 0 \\ \cos h_S \end{pmatrix}$$

Since for other points of the sun's disk the difference between $\vec{e}_0$ and $\vec{e}_{00}$ is small, $\vec{e}_{0,0°}$ and $\vec{e}_{0,90°}$ differ only slightly from the directions for the central point as well.

The 45° directions are simply given by:

$$\vec{e}_{0,45°} = \frac{1}{\sqrt{2}} \cdot \left(\vec{e}_{0,0°} + \vec{e}_{0,90°}\right) \qquad \text{and} \qquad \vec{e}_{0,-45°} = \frac{1}{\sqrt{2}} \cdot \left(\vec{e}_{0,0°} - \vec{e}_{0,90°}\right)$$

These relations hold true for any polarization coordinate system, which implies that $\vec{e}_{0°}$ and $\vec{e}_{90°}$ contain all necessary information.

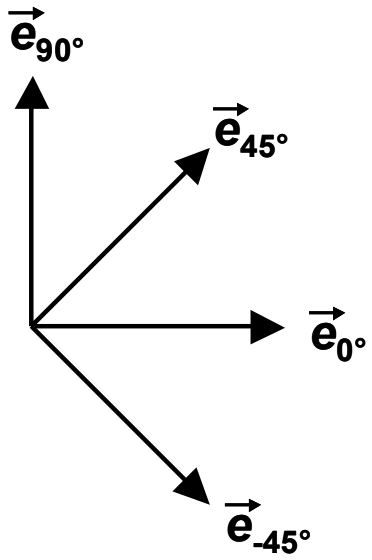

Fig. S2: A set of unit vectors describing the rotation directions of a polarizer for measuring the polarized intensities needed to calculate the Stokes vector components S_1 and S_2.

It is convenient to set the S_0 component of the initial Stokes vector to 1 ("normalized Stokes vector"), as absolute intensity calculations are not the aim of this simulation study. For natural (unpolarized) sunlight, the initial normalized Stokes vector is then simply given by

$$\vec{S}_{00} = \begin{pmatrix} 1 \\ 0 \\ 0 \\ 0 \end{pmatrix}$$

Within this naming convention, the first zero stands for the $(\vec{e}_{0,0°}, \vec{e}_{0,90°})$ polarization reference frame and the second zero indicates the initial state before any interaction with the drop.

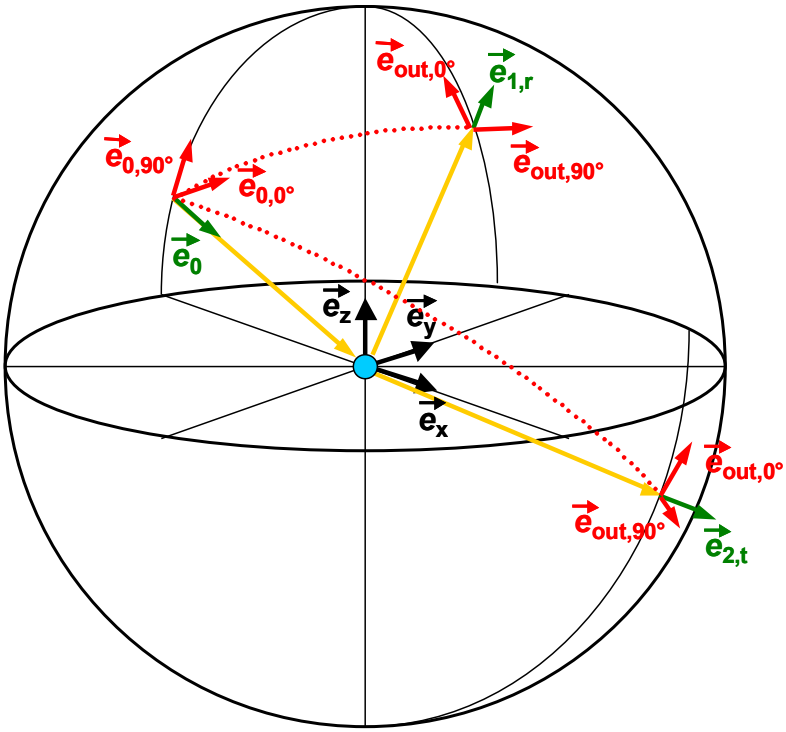

Fig. S3: Schematic view of the polarization coordinate systems for the incoming ray $\vec{e}_0$ *and the exiting rays* $\vec{e}_{1,r}$ *and* $\vec{e}_{2,t}$ *(*$\vec{e}_{3,t} \ldots \vec{e}_{7,t}$ *are treated analogously, if they exist*). *For the incoming ray, the direction towards the zenith specifies* $\vec{e}_{0,0°}$. *For the outgoing rays,* $\vec{e}_{out,90°}$ *points always towards to the antisolar point, allowing to work with azimuthal and radial polarization at each point on the celestial sphere.*

It would not be necessary to specify $\vec{e}_{0,0°}$ and $\vec{e}_{0,90°}$ if only the case of unpolarized incident light is to be modeled. However, partially or totally polarized incident light may occur in nature when the sunlight is first reflected at a water surface and then reaches the drop (reflected-light rainbows). Defining a proper reference frame from the beginning allows to treat such situations with the present model as well.

6. First Stokes vector rotation

Stokes vectors for light reflected and transmitted at a dielectric interface can be calculated from the incident Stokes vector using the Müller matrix formalism, which in this case includes Fresnel's formulas as well. The respective Müller matrices are, however, constructed for the "natural" polarization reference frame at the interface, i.e. the incidence plane. This means, before reflection and transmission can be treated, the initial Stokes vector has to be

transformed into the incidence plane polarization coordinates. The respective unit vectors for this coordinate system are given by

$$\vec{e}_{1,0^\circ} = \frac{\vec{n}_1 \times \vec{e}_0}{\left|\vec{n}_1 \times \vec{e}_0\right|} \qquad \text{TE polarization (s polarization)}$$

$$\vec{e}_{10,90^\circ} = \vec{e}_0 \times \vec{e}_{1,0^\circ} \qquad \text{TM polarization (p polarization)}$$

$\vec{e}_{1,0^\circ}$ describes the 0° direction (TE polarization) not only for the incident ray, but also for the reflected and transmitted rays. Contrasting to this, the 90° direction (TM polarization) differs for these three situations: $\vec{e}_{10,90^\circ}$ serves this purpose for the incident ray hitting the drop at $\vec{r}_1$, whereas $\vec{e}_{11r,90^\circ} = \vec{e}_{1,r} \times \vec{e}_{1,0^\circ}$ and $\vec{e}_{11t,90^\circ} = \vec{e}_{1,t} \times \vec{e}_{1,0^\circ}$ are the corresponding directions for the reflected and transmitted rays, with their propagation directions being given by $\vec{e}_{1,r}$ and $\vec{e}_{1,t}$, respectively (see below).

The old and new polarization coordinates are rotated by the angle ϑ_{10} with respect to each other (see Fig. S4):

$$\cos\vartheta_{10} = \vec{e}_{1,0^\circ} \cdot \vec{e}_{0,0^\circ}$$

$$\sin\vartheta_{10} = \cos\left(\frac{\pi}{2} - \vartheta_{10}\right) = \vec{e}_{1,0^\circ} \cdot \vec{e}_{0,90^\circ}$$

As these two independent angular functions can be calculated from the known unit vectors, ϑ_{10} can be uniquely determined within the interval $-\pi$ to $+\pi$ (or 0 to 2π, which makes no difference).

The rotation matrix and the rotated Stokes vector are then given by [57]:

$$\underline{M}_{rot10} = \begin{pmatrix} 1 & 0 & 0 & 0 \\ 0 & \cos 2\vartheta_{10} & \sin 2\vartheta_{10} & 0 \\ 0 & -\sin 2\vartheta_{10} & \cos 2\vartheta_{10} & 0 \\ 0 & 0 & 0 & 1 \end{pmatrix}$$

$$\vec{S}_{10} = \underline{M}_{rot10} \cdot \vec{S}_{00}$$

Note that the rotation affects only the S_1 and S_2 component, as S_0 (total intensity) and S_3 (amount of circular polarization) are independent from the reference system.

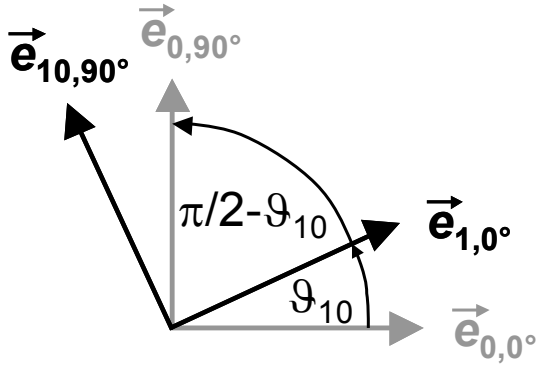

Fig. S4: Orientation relation between the initial polarization coordinate system for the incident ray ("old" system, gray) and the coordinate system attached to the incidence plane at $\vec{r}_1$ ("new" system, black). The cosines of the marked angles are accessible by scalar products of the involved unit vectors.

7. First reflection and transmission

The law of reflection and Snell's law can be formulated in terms of unit vectors describing the propagation directions:

$$q_1 = \vec{e}_0 \cdot \vec{n}_1$$

$$\vec{e}_{1,r} = \vec{e}_0 - 2q_1 \cdot \vec{n}_1 \qquad \text{reflection}$$

$$\vec{e}_{1,t} = \frac{\vec{e}_0}{n} + \left(\sqrt{1 - \frac{1-q_1^2}{n^2}} - \frac{q_1}{n} \right) \cdot \vec{n}_1 \qquad \text{transmission}$$

(n : refractive index of water for the chosen wavelength)

The Müller matrices for both these transitions can be calculated the following way [57]:

$$\vartheta_i = \arccos(q_1) \qquad \text{angle of incidence}$$

$$\vartheta_r = \arcsin\left(\frac{\sin \vartheta_i}{n} \right) \qquad \text{angle of refraction}$$

$$\vartheta_+ = \vartheta_i + \vartheta_r$$

$$\vartheta_- = \vartheta_i - \vartheta_r$$

$$\underline{M}_{1r} = \frac{1}{2}\left(\frac{\tan\vartheta_-}{\sin\vartheta_+}\right)^2 \cdot \begin{pmatrix} \cos^2\vartheta_- + \cos^2\vartheta_+ & \cos^2\vartheta_- - \cos^2\vartheta_+ & 0 & 0 \\ \cos^2\vartheta_- - \cos^2\vartheta_+ & \cos^2\vartheta_- + \cos^2\vartheta_+ & 0 & 0 \\ 0 & 0 & -2\cos\vartheta_+\cos\vartheta_- & 0 \\ 0 & 0 & 0 & -2\cos\vartheta_+\cos\vartheta_- \end{pmatrix}$$

$$\underline{M}_{1t} = \frac{\sin 2\vartheta_i \cdot \sin 2\vartheta_r}{2\left(\sin\vartheta_+\cos\vartheta_-\right)^2} \cdot \begin{pmatrix} \cos^2\vartheta_- + 1 & \cos^2\vartheta_- - 1 & 0 & 0 \\ \cos^2\vartheta_- - 1 & \cos^2\vartheta_- + 1 & 0 & 0 \\ 0 & 0 & 2\cos\vartheta_- & 0 \\ 0 & 0 & 0 & 2\cos\vartheta_- \end{pmatrix}$$

The reflected and transmitted Stokes vectors in the incidence plane reference frame are then:

$$\vec{S}_{11t} = \underline{M}_{1t} \cdot \vec{S}_{10}$$

$$\vec{S}_{11r} = \underline{M}_{1r} \cdot \vec{S}_{10}$$

8. Stokes vector rotation for the exiting ray

The reflected ray propagating in the direction $\vec{e}_{1,r}$ leaves the drop and thus constitutes the $p = 0$ contribution [59, 60] to its scattering light pattern. From the components of $\vec{e}_{1,r}$, azimuth and elevation in the laboratory system are calculated, spatially inverted to account for the "sky transform" (see main document and [23]) and assigned to a pixel within the final Stokes component image stack, e.g. in a sun-centered Lambert projection.

However, $\vec{S}_{11r}$ is again not directly suited to be recorded in this image stack, as it is still referenced to the incidence plane of the first piercing point. It must first be transformed into an useful external polarization coordinate system independent of the direction of $\vec{n}_1$. This is constructed as follows:

$$\vec{e}_{out,0^\circ} = \frac{\vec{e}_{00} \times \vec{e}_{1,r}}{\left|\vec{e}_{00} \times \vec{e}_{1,r}\right|} \qquad \text{and} \qquad \vec{e}_{out,90^\circ} = \vec{e}_{1,r} \times \vec{e}_{out,0^\circ}$$

As seen from Fig. S3, $\vec{e}_{out,0^\circ}$ corresponds to the azimuthal and $\vec{e}_{out,90^\circ}$ to the radial polarization direction with respect to the central point of the sun's disk for every point on the celestial sphere (with the exception of the two singular poles in and against the $\vec{e}_{00}$ direction).

Illustratively said, $\vec{e}_{out,90°}$ is constructed to point directly to the antisolar point and $\vec{e}_{out,0°}$ points in the perpendicular direction.

The Stokes vector rotation is accomplished basically in the same way as described in section 6. It is however more convenient to calculate the sine of the rotation angle from a different scalar product (see also Fig. S5):

$$\cos\vartheta_{out,1} = \vec{e}_{out,0°} \cdot \vec{e}_{1,0°}$$

$$\sin\vartheta_{out,1} = -\vec{e}_{out,90°} \cdot \vec{e}_{1,0°} \qquad \left(\text{as } \cos\left(\frac{\pi}{2} + \vartheta_{out,1}\right) = \vec{e}_{out,90°} \cdot \vec{e}_{1,0°}\right)$$

$$\underline{M}_{rot,out,1} = \begin{pmatrix} 1 & 0 & 0 & 0 \\ 0 & \cos 2\vartheta_{out,1} & \sin 2\vartheta_{out,1} & 0 \\ 0 & -\sin 2\vartheta_{out,1} & \cos 2\vartheta_{out,1} & 0 \\ 0 & 0 & 0 & 1 \end{pmatrix}$$

$$\vec{S}_{out,1} = \underline{M}_{rot,out,1} \cdot \vec{S}_{11r}$$

The four components of $\vec{S}_{out,1}$ are then added up to the previous entries of the respective projection maps' pixels. The total data array contains further dimensional layers for the 18 different wavelengths and the number of interactions with the drop (given by $p+1$, with $p=1$ corresponding to direct transmission, $p=2$ to the primary rainbow order, $p=3$ to the secondary and so on).

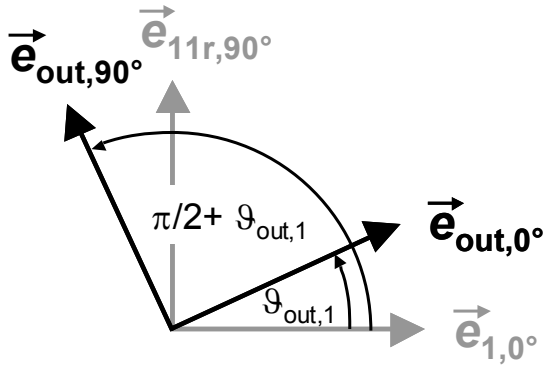

Fig. S5: Orientation relation between the polarization coordinate system attached to the incidence plane at $\vec{r}_1$ for the externally reflected ray $\vec{e}_{1,r}$ ("old" system, gray) and the external azimuthal/radial reference frame ("new" system, black).

9. Reflection and transmission at second and subsequent piercing points

From $\vec{r}_1$ and $\vec{e}_{1,t}$, the second piercing point $\vec{r}_2$ is calculated using the defining equations of the 2HS surface, again paying attention to the proper case discrimination. The normal vector at this (and similarly at all subsequent) piercing points is given by:

$$\vec{N}_2 = \begin{pmatrix} x_2 \\ y_2 \\ a/b_{1,2} \cdot z_2 \end{pmatrix} \qquad \vec{n}_2 = + \frac{\vec{N}_2}{\left|\vec{N}_2\right|}$$

In contrast to $\vec{n}_1$, $\vec{n}_2$ is constructed to point outward of the drop, i.e. into the half space of the transmitted ray, if such exists (see Fig. S1).

The polarization coordinate system for incidence at $\vec{r}_2$ is:

$\vec{e}_{2,0^\circ} = \dfrac{\vec{n}_2 \times \vec{e}_{1,t}}{\left|\vec{n}_2 \times \vec{e}_{1,t}\right|}$ TE polarization (s polarization) for incidence, reflection, and (if possible) transmission

$\vec{e}_{21,90^\circ} = \vec{e}_{1,t} \times \vec{e}_{2,0^\circ}$ TM polarization (p polarization) for incidence

The rotation angle between this and the previous reference frame for transmission at $\vec{r}_1$ can again be determined from

$$\cos \vartheta_{21} = \vec{e}_{2,0^\circ} \cdot \vec{e}_{1,0^\circ}$$

$$\sin \vartheta_{21} = -\vec{e}_{21,90^\circ} \cdot \vec{e}_{1,0^\circ}$$

with the usual construction of the rotation matrix as discussed in section 6:

$$\vec{S}_{21} = \underline{M}_{rot\,21} \cdot \vec{S}_{11t}$$

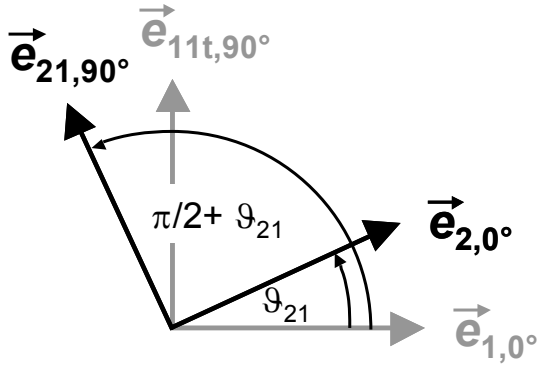

Fig. S6: Orientation relation between the polarization coordinate system attached to the incidence plane at $\vec{r}_1$ for the transmitted ray $\vec{e}_{1,t}$ ("old" system, gray) and the coordinate system attached to the incidence plane at $\vec{r}_2$ ("new" system, black).

Note that ϑ_{21} and all subsequent of these internal rotation angles are zero in case of a spherical drop, in which the ray path is confined to a single plane. As this symmetry is broken for the distorted drop shape, the nonzero $S_{11t,1}$ component, which arises for unpolarized incident light due to the transmission at $\vec{r}_1$ (as described by Fresnel's formulas), can be transformed into a non-zero $S_{21,2}$ component without any change of the physical polarization state as seen from the viewpoint of the laboratory system, being caused only by the twist between the two planes of incidence at $\vec{r}_1$ and $\vec{r}_2$.

The direction of the internally reflected ray is calculated the same way as described in section 7:

$$q_2 = \vec{e}_{1,t} \cdot \vec{n}_2$$

$$\vec{e}_{2,r} = \vec{e}_{1,t} - 2q_2 \cdot \vec{n}_2 \qquad \text{(internal reflection)}$$

Case A: Non-total internal reflection

If $\left(1-q_2^2\right)\cdot n^2 < 1$, no total internal reflection occurs and the ray transmitted out of the drop propagates in the direction:

$$\vec{e}_{2,t} = \vec{e}_{1,t} \cdot n + \left(\sqrt{1-\left(1-q_2^2\right)\cdot n^2} - q_2 \cdot n\right)\cdot \vec{n}_2$$

The Müller matrices for reflection and transmission are then also calculated analogously to section 7, and yield the reflected and transmitted Stokes vectors in the incidence plane reference frame:

$$\vec{S}_{22t} = \underline{M}_{2t} \cdot \vec{S}_{21}$$

$$\vec{S}_{22r} = \underline{M}_{2r} \cdot \vec{S}_{21}$$

Like in section 8, the external polarization vectors are afterwards calculated for the exiting ray (see Fig. S3), the angle of rotation is determined and the transmitted Stokes vector is transformed and recorded:

$$\vec{e}_{out,0°} = \frac{\vec{e}_{00} \times \vec{e}_{2,t}}{\left|\vec{e}_{00} \times \vec{e}_{2,t}\right|} \qquad \text{and} \qquad \vec{e}_{out,90°} = \vec{e}_{2,t} \times \vec{e}_{out,0°}$$

$$\cos \vartheta_{out,2} = \vec{e}_{out,0°} \cdot \vec{e}_{2,0°}$$

$$\sin \vartheta_{out,2} = -\vec{e}_{out,90°} \cdot \vec{e}_{2,0°}$$

$$\vec{S}_{out,2} = \underline{M}_{rot,out,2} \cdot \vec{S}_{22t}$$

Case B: Total internal reflection (TIR)

If $\left(1 - q_2^2\right) \cdot n^2 \geq 1$, no transmitted ray exists, i.e. $\underline{M}_{2t} = 0$, $\vec{S}_{22t} = 0$ and $\vec{S}_{out,2} = 0$.

The Müller matrix for TIR is not simply the unit matrix, as a phase shift occurs between TE and TM polarization, resulting in an elliptic polarization of the reflected light in the general case. This relative phase shift $\delta \,(= \delta_S - \delta_P)$ is given by [57]:

$$\tan \frac{\delta}{2} = -\frac{\cos \vartheta_i \cdot \sqrt{n^2 \cdot \sin^2 \vartheta_i - 1}}{n \cdot \sin^2 \vartheta_i}$$

The phase shift departs from zero for ϑ_i equal to the critical angle of TIR, reaches a (negative) maximum value of $\tan \frac{\delta_{\max}}{2} = -\frac{n^2 - 1}{2n}$ [66] and drops again to zero as ϑ_i approaches 90°. For $n = 1.34$, $\delta_{\max}$ is about -33.1°.

The Müller matrix for reflection and the Stokes vector are calculated as follows:

$$\underline{M}_{2r} = \begin{pmatrix} 1 & 0 & 0 & 0 \\ 0 & 1 & 0 & 0 \\ 0 & 0 & \cos\delta & -\sin\delta \\ 0 & 0 & \sin\delta & \cos\delta \end{pmatrix}$$

$$\vec{S}_{22r} = \underline{M}_{2r} \cdot \vec{S}_{21}$$

From the structure of $\underline{M}_{2r}$ it is clear that a nonzero $S_{21,2}$ component can be transformed into a nonzero $S_{22r,3}$ value. For the primary rainbow, this is the only way to generate an elliptically polarized output (which would then occur in the direction $\vec{e}_{3,t}$), as only one internal reflection occurs along its ray path, which has then to be necessarily total. This means that the elliptically polarized light is "robbed" from the zero order glow ($\vec{e}_{2,t}$, which does not exist in this case). Higher rainbow orders are more difficult to discuss due to the multiple internal reflections, which may be total or not; however, the chance to generate elliptically polarized light increases with the rainbow order.

Independent whether the reflection at $\vec{r}_2$ is total or not, the ray propagating in $\vec{e}_{2,r}$ direction with its intensity and polarization state described by $\vec{S}_{22r}$ is further traced inside the drop. The subsequent piercing points up to $\vec{r}_7$ for the quinary rainbow are calculated analogously by employing the laws of reflection and refraction, thereby unveiling successively at which points on the celestial sphere the contributions to the respective rainbow orders are located. Simultaneously, the Stokes vector evolution is monitored by applying the proper rotation and Müller matrices.

Additional references

[66] R. M. A. Azzam, "Phase shifts that accompany total internal reflection at a dielectric–dielectric interface," J. Opt. Soc. Am. A **21**, 1559-1563 (2004).

Part II: Sun disk convolution for DMK simulations

In the DMK simulations, a problem arises at a rather early stage, i.e. before applying the Möbius shifts: The Debye series algorithm [15] produces results which are valid only for an incident plane wave, i.e. a point-like light source at infinite distance. Though an individual point on the sun can be regarded as infinitely far for this purpose, the problem remains how to deal with multitude of emission points on the earthward side of the sun that produce plane waves arriving from different directions at the observer, i.e. the finite angular size of the sun.

This difficulty is not only relevant for rainbow simulations, but also for the theoretical treatment of many other effects in atmospheric optics (and beyond). Mostly this procedure is just briefly mentioned as "convolution with the sun's disk" but details are seldom provided. To precisely state the problem, the following definitions may be proposed:

ϑ: scattering angle to the point of observation, either (1) from a point light source or (2) from the center of a disk-like extended source, with $0 \le \vartheta \le \pi$.

$I(\vartheta)$: rotational symmetric scattering light intensity for point source (e.g. Debye series data after taking the absolute square of the amplitude). The rotational symmetry is manifested by the fact that I does not depend on the clock angle.

Ω_S solid angle size of the round, disk-like light source with homogenous emission from every solid angle element on this disk. To simplify the language, this will be further referred to as "the sun" - though it could also be the moon or, under certain circumstances, also a terrestrial light source. It should be noted that both the sun and the moon might the requirements only approximately, as the sun gets slightly darker towards the edge and the moon has an albedo variation due to its topography.

For the sun's solid angle, one obtains $\Omega_S = 2\pi(1-\cos r_S)$. This yields $\Omega_S = 7.0 \cdot 10^{-5}$ for an angular radius of $r_S = 0.27°$.

The task is now to calculate the quantity:

$\bar{I}(\vartheta)$: rotational symmetric scattering light intensity given by integration of $I(\vartheta)$ over the sun's disk. Assuming incoherence between the emitted waves from different points of the sun's disks, the respective intensities (not amplitudes) have to be summed up. For

convenience, also the normalization shall be kept, i.e. integration of $\bar{I}(\vartheta)$ over the full celestial sphere shall yield the same result as the integration of $I(\vartheta)$.

From intuition, one expects that the result might be written as a one-dimensional convolution in the scattering angle, i.e.:

$$\bar{I}(\vartheta) = \int_{-r_S}^{r_S} d\delta \cdot I(\vartheta + \delta) \cdot f(\delta)$$

The convolution kernel $f(\delta)$ should somehow resemble the circular shape of the sun's disk, hence it would be natural to choose a half circle ranging from $-r_S \le \delta \le r_S$. Of course, such an assumption requires an appropriate proof, moreover, it is yet unclear how to deal with very small ($\vartheta \le r_S$) and very large scattering angles ($\vartheta \ge \pi - r_S$), as the allowed range for the argument of $I(\vartheta + \delta)$ will be exceeded in the integral.

An exact solution for this problem can be obtained as follows. It may further be defined:

ϑ_1, φ_1: point-of-observation-centered angular coordinates (polar angle, azimuth), used to describe the location of points on the sun's disk. $\varphi_1 = 0$ may describe the direction towards the sun's center.

In these coordinates, a differential solid angle element of the sun's disk is given by:

$$d\Omega = \sin\vartheta_1 \cdot d\vartheta_1 \cdot d\varphi_1$$

The straightforward solution for $\bar{I}(\vartheta)$ can then be written as a two-dimensional integral over ϑ_1 and φ_1 in the appropriate limits given by the solar disk's edge (see Fig. S7):

$$\bar{I}(\vartheta) = \frac{1}{\Omega_S} \cdot \int_{\vartheta_{1\min}(\theta)}^{\vartheta_{1\max}(\vartheta)} d\vartheta_1 \int_{\varphi_{1\min}(\vartheta,\vartheta_1)}^{\varphi_{1\max}(\vartheta,\vartheta_1)} d\varphi_1 \cdot \sin\vartheta_1 \cdot I(\vartheta_1)$$

As the emitted power per solid angle element is assumed to be constant, the integration over φ_1 is trivial and yields the difference between upper and lower limit as an additional factor. Since $\varphi_{1\min} = -\varphi_{1\max}$, this reduces to:

$$\bar{I}(\vartheta) = \frac{2}{\Omega_S} \cdot \int_{\vartheta_{1\min}(\vartheta)}^{\vartheta_{1\max}(\vartheta)} d\vartheta_1 \cdot \varphi_{1\max}(\vartheta,\vartheta_1) \cdot \sin\vartheta_1 \cdot I(\vartheta_1)$$

To reach the goal of a simple convolution formulation, $\varphi_{1\max}(\vartheta,\vartheta_1)$ as well as the integration limits $\vartheta_{1\max}(\vartheta)$ and $\vartheta_{1\min}(\vartheta)$ must be determined, which requires the following case discrimination:

Case A : $r_S \le \vartheta \le \pi - r_S$ ("most of the sky")

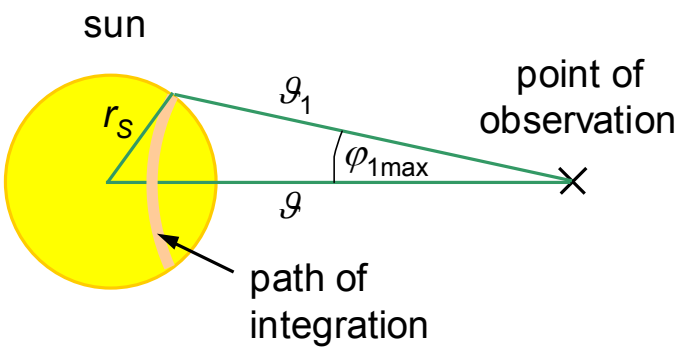

Fig. S7: Integration geometry for Case A

From the spherical law of cosines, one obtains the relation (see Fig. S7):

$$\cos r_S = \cos\vartheta\cos\vartheta_1 + \sin\vartheta\sin\vartheta_1\cos\varphi_{1\max}$$

This gives rearranged:

$$\varphi_{1\max} = \arccos\left(\frac{\cos r_S - \cos\vartheta\cos\vartheta_1}{\sin\vartheta\sin\vartheta_1}\right)$$

The limits are $\vartheta_{1\max} = \vartheta + r_S$ and $\vartheta_{1\min} = \vartheta - r_S$.

Case B : $\vartheta < r_S$

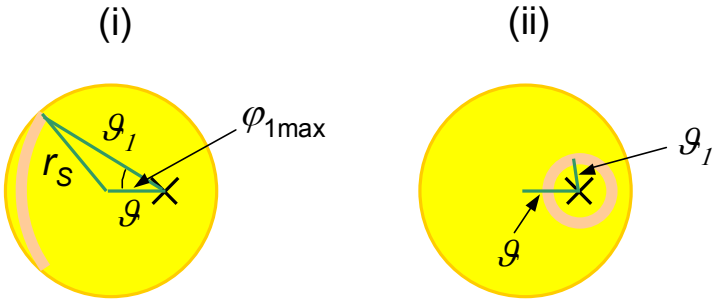

Fig. S8: Integration geometries for Case B

A further sub-case discrimination is necessary, as the integration path undergoes a qualitative transition to a full circle (see Fig. S8):

B (i): $\vartheta_1 > r_S - \vartheta$: $\varphi_{1\max} = \arccos\left(\frac{\cos r_S - \cos\vartheta\cos\vartheta_1}{\sin\vartheta\sin\vartheta_1} \right)$

B (ii): $\vartheta_1 \le r_S - \vartheta$: $\varphi_{1\max} = \pi$

The limits are $\vartheta_{1\max} = \vartheta + r_S$ and $\vartheta_{1\min} = 0$.

Case C: $\vartheta > \pi - r_S$

C (i): $\vartheta_1 < 2\pi - \vartheta - r_S$: $\varphi_{1\max} = \arccos\left(\frac{\cos r_S - \cos\vartheta\cos\vartheta_1}{\sin\vartheta\sin\vartheta_1} \right)$

C (ii): $\vartheta_1 \ge 2\pi - \vartheta - r_S$: $\varphi_{1\max} = \pi$

The limits are $\vartheta_{1\max} = \pi$ and $\vartheta_{1\min} = \vartheta - r_S$.

Summary

It is possible to formulate $\bar{I}(\vartheta)$ in the desired way as a convolution, though the kernel turns out to be more complicated as might be expected. The result reads as:

$$\bar{I}(\vartheta) = \int_{\delta_{\min}}^{\delta_{\max}} d\delta \cdot I(\vartheta + \delta) \cdot f_\vartheta(\delta)$$

The convolution kernel depends itself on ϑ:

$$f_\vartheta(\delta) = \frac{1}{\pi(1 - \cos r_S)} \cdot \sin(\vartheta + \delta) \cdot \varphi_{1\max}(\vartheta, \delta)$$

In that expression, $\varphi_{1\max}(\vartheta, \delta)$ is given by:

$$c = \frac{\cos r_S - \cos\vartheta\cos(\vartheta + \delta)}{\sin\vartheta\sin(\vartheta + \delta)}$$

if $c > -1$: $\varphi_{1\max} = \arccos c$, else $\varphi_{1\max} = \pi$

The integration limits are:

Case A: $r_S \le \vartheta \le \pi - r_S$ $\delta_{\min} = -r_S$, $\delta_{\max} = r_S$

Case B: $\vartheta < r_S$ $\delta_{\min} = -\vartheta$, $\delta_{\max} = r_S$

Case C: $\vartheta > \pi - r_S$ $\delta_{\min} = -r_S$, $\delta_{\max} = \pi - \vartheta$

Though it seems unlikely that this result can be further simplified in the general case, it is straightforward to show that for $\vartheta = \pi/2$ and $r_S << 1$ (which is a Case A situation), one obtains by approximating the angular functions with their Taylor expansions truncated after their respective first non-trivial terms:

$$f_\vartheta(\delta) \approx \frac{2}{\pi \cdot r_S^2} \cdot \sqrt{r_S^2 - \delta^2}$$

This is the intuitively expected half-circle kernel. For other scattering angles, this shape will be exceedingly distorted, as either the sun or the antisolar point are approached.

In the present DMK simulations, the Debye series data are sampled at 0.05° intervals in the scattering angle, and the convolution integral is approximated by a discrete summation over the roughly 10 grid points that correspond to the sun's angular diameter.